Biogeosciences Discuss., 9, 15699–15722, 2012
www.biogeosciences-discuss.net/9/15699/2012/
doi:10.5194/bgd-9-15699-2012

Biogeosciences
Discussions

Stable isotope and modelling evidence that CO_2 drives vegetation changes in the tropics

F. J. Bragg[1,2], I. C. Prentice[1,3,4], S. P. Harrison[2,3], G. Eglinton[1,5,6], P. N. Foster[1], F. Rommerskirchen[7,8], and J. Rullkötter[7]

[1]Department of Earth Sciences, University of Bristol, Wills Memorial Building, Bristol BS8 1RJ, UK
[2]School of Geographical Sciences, University of Bristol, Bristol BS8 1SS, UK
[3]Department of Biological Sciences, Macquarie University, North Ryde, NSW 2109, Australia
[4]Grantham Institute and Division of Ecology and Evolution, Imperial College, Silwood Park Campus, Ascot SL5 7PY, UK
[5]Dartmouth College, Hanover, NH 03755, USA
[6]Department of Marine Chemistry and Geochemistry, Woods Hole Oceanographic Institution, 266 Woods Hole Road, Woods Hole, MA 02543-1050, USA
[7]Institute for Chemistry and Biology of the Marine Environment (ICBM), Carl von Ossietzky University of Oldenburg, P.O. Box 2503, 26111 Oldenburg, Germany
[8]MARUM, University of Bremen, Leobener Straße, 28359 Bremen, Germany

Received: 19 June 2012 – Accepted: 15 September 2012 – Published: 9 November 2012

Correspondence to: I. C. Prentice (colin.prentice@mq.edu.au)

Published by Copernicus Publications on behalf of the European Geosciences Union.

Abstract

Atmospheric CO_2 concentration is hypothesized to influence vegetation distribution via tree-grass competition, with higher CO_2 concentrations favouring trees. The stable carbon isotope ($\delta^{13}C$) signature of vegetation is influenced by the relative importance of C_4 plants (including most tropical grasses) and C_3 plants (including nearly all trees), and the degree of stomatal closure – a response to aridity – in C_3 plants. Compound-specific $\delta^{13}C$ analyses of leaf-wax biomarkers in sediment cores of an offshore South Atlantic transect are used here as a record of vegetation changes in subequatorial Africa. These data suggest a large increase in C_3 relative to C_4 plant dominance after the Last Glacial Maximum. Using a process-based biogeography model that explicitly simulates ^{13}C discrimination, we show that climate change alone cannot explain the observed shift in $\delta^{13}C$ values. The physiological effect of increasing CO_2 concentration is decisive, altering the C_3/C_4 balance and bringing the simulated and observed $\delta^{13}C$ values into line.

It is concluded that CO_2 concentration itself was a key agent of tropical vegetation change during the last glacial-interglacial transition. Two additional inferences follow. First, long-term variations in terrestrial $\delta^{13}C$ values are not simply a proxy for regional rainfall as has sometimes been assumed. Such interpretations need to be re-examined. Second, rising CO_2 concentration today is likely to be influencing tree-grass competition in a similar way, and thus contributing to the "woody thickening" observed in savannas worldwide. This second inference points to the importance of experiments to determine how vegetation composition in savannas is likely to be influenced by the continuing rise in CO_2 concentration.

1 Introduction

The effects of changes in atmospheric CO_2 concentration on vegetation composition and biome distribution have received relatively little attention, compared with its effects on primary productivity (Ainsworth and Piao, 2005; Norby et al., 2005) and the terrestrial carbon sink (Prentice et al., 2001; Friedlingstein et al., 2006). Rising CO_2 has however been suggested as one potential cause of "woody thickening". Woody thickening is the widely observed increase of tree and shrub density in savannas (Prentice et al., 2001; Archer et al., 1995, 2001; Bond and Midgely, 2000; MacInnis-Ng et al., 2011). Rising CO_2 over the last glacial-interglacial transition has also been proposed as a major cause of the worldwide increase in forest cover shown by pollen records (Street-Perrott et al., 1997; Jolly and Haxeltine, 1997; Cowling, 1999; Cowling and Sykes, 1999; Bond et al., 2003; Harrison and Prentice, 2003; Cowling and Shin, 2006).

Increasing CO_2 concentration would be expected to favour trees over grasses by increasing the growth rates of (C_3) trees relative to tropical (C_4) grasses, which are less responsive to CO_2 (Ehleringer et al., 1997); and more generally, by allowing faster-growing tree seedlings to escape the "fire trap" in fire-prone grasslands and savannas (Bond and Midgley, 2000; Bond et al., 2008; Kgope et al., 2010). Global vegetation models consistently predict that increasing CO_2 concentration should favour trees, especially but not exclusively in the tropics, both during the transition from the Last Glacial Maximum (LGM) to the Holocene and under present conditions of rising CO_2 (Bond and Midgely, 2000; Bond et al., 2003; Harrison and Prentice, 2003; Prentice and Harrison, 2009; Prentice et al., 2011a). Global modelling has also shown that physiological effects of the change in CO_2 concentration over the last deglaciation must be considered in order to reproduce the increase in forest cover shown by pollen records (Harrison and Prentice, 2003; Prentice and Harrison, 2009).

Pollen analysis provides the most abundant data on past vegetation globally, but pollen records are relatively sparse in the tropics and southern hemisphere. An additional, spatially integrated vegetation "sensor" is provided by stable carbon isotope ($\delta^{13}C$) analysis of plant debris and residues (Eglinton and Eglinton, 2008; Zhao et al., 2003): in particular, compound-specific $\delta^{13}C$ analysis of *n*-alkanes in offshore marine sediments. Long-chain *n*-alkanes are of terrestrial origin (Pearson and Eglinton, 2000). They are deflated and abraded from the waxy cuticles of vascular plants and transported to the marine environment directly and in soil and dust particles by the prevailing winds, and more locally by rivers. The δ^{13}C values of plant material are strongly dependent on the photosynthetic pathway (Farquhar et al., 1982; Farquhar, 1983). C_4 plants discriminate against ^{13}C by ~ 4 to 8 ‰ and C_3 plants by ~ 14 to 24 ‰. The range of values for C_3 plants reflects the influence of aridity, as discrimination by C_3 photosynthesis is weaker under drier conditions due to stomatal closure (Farquhar et al., 1982; Lloyd and Farquhar, 1994; Diefendorf et al., 2010; Prentice et al., 2011b). The stable carbon isotope signature of cuticular *n*-alkanes reflects that of the total leaf lipids from which they originated, with an average offset of −6 ‰ for C_3 vegetation and −10 ‰ for C_4 vegetation (Collister et al., 1994). To first order, changes in the δ^{13}C of these biomarkers thus indicate changes in the balance of C_3 and C_4 plants in the source vegetation, with less negative values indicating more C_4 plants. This signal is overprinted by an effect of aridity on C_3 photosynthesis: for a given ratio of C_3 to C_4 foliage biomass, less negative values imply a drier environment.

Here we use a data set (Rommerskirchen et al., 2006) of *n*-alkane δ^{13}C measurements from sediments corresponding to the period around the LGM (Marine Isotope Stage 2, MIS 2) and the Holocene (Marine Isotope Stage 1, MIS 1), taken along a meridional transect of marine cores to the west of subequatorial Africa in Fig. 1. The data show similar values for δ^{13}C in MIS 1 and 2 south of about 20° S. Between the equator and 20° S, however, the values for the two periods differ by up to 5 ‰. This difference has been used to suggest a substantially greater vegetation representation of C_4 plants in tropical Africa during MIS 2, which in turn would imply a major expansion of tropical forests at the expense of C_4 grasslands during the transition from the LGM to the Holocene (Rommerskirchen et al., 2006). Additional, supporting latitudinal δ^{13}C data on leaf-wax *n*-alkanes in southeastern Atlantic Ocean sediments have recently been obtained by Vogts (2011) and Vogts et al. (2012) who sampled an isobathic transect of surface sediments from 1° N to 28° S. The *n*-C_{29-33} weighted mean average δ^{13}C values increased from −33 ‰ in the north to around −26 ‰ in the south. The latitudinal trend and absolute δ^{13}C values of the *n*-alkanes along this 13-site transect

(~1300 m water depth) closely match those of the 9-site Holocene transect (738 to 3973 m water depth) as shown in Fig. 1. We combine climate model simulations of LGM and Holocene climates with a state-of-the-art biogeography model, which explicitly simulates the C_3/C_4 equilibrium and ^{13}C discrimination by plants, in order to quantify the contributions of climate change and physiological CO_2 effects in driving the observed large temporal shift in $\delta^{13}C$ values in the tropical part of the transect.

2 Methods

We used recent climate data and Palaeoclimate Modelling Intercomparison Project (PMIP) Phase 2 simulations of the global climate (Braconnot et al., 2007) during the mid-Holocene, MH (defined as 6000 yr before present) and the LGM (21 000 yr before present), to drive the state-of-the-art coupled equilibrium biogeochemistry-biogeography model, BIOME4 (Kaplan, 2001; Kaplan et al., 2003). Trajectory analysis was used to estimate probabilities of different contributing source areas for deflated plant material in each marine core. Simulated $\delta^{13}C$ values at contributing grid cells were then averaged with weighting according to leaf area index (representing the surface area of deflatable material) and estimated source probability.

2.1 Climate model simulations

The PMIP MH climate simulations include the effects of changing orbital parameters, affecting the seasonal and latitudinal distribution of insolation, during the Holocene. They were driven with pre-industrial CO_2 concentration (280 ppm) while methane concentration was reduced, following the PMIP Phase 2 protocol. The PMIP LGM climate simulations include orbital parameters closer to today's, but impose large continental ice-sheets specified from ICE5G (Peltier, 2004) and reduced atmospheric concentrations of the three long-lived biogenic greenhouse gases (methane, nitrous oxide and CO_2). LGM climate model simulations, combined with biosphere models, can reproduce the broad-scale global patterns of glacial-interglacial vegetation changes (as shown by pollen data) provided physiological effects of changing CO_2 concentration are taken into account (Harrison and Prentice, 2003; Prentice et al., 2011a). We used the ECHAM, FGOALS, FOAM, IPSL, MIROC, MRI-fa, MRI-nfa and UBRIS model simulations for the MH and the FGOALS, HadCM3, IPSL and MIROC model simulations for the LGM. These were the models whose outputs were available in the PMIP archive, http://pmip2.lsce.ipsl.fr/, and provided all of the model output fields required to drive BIOME4, at the time when the archive was accessed.

2.2 Biogeography model simulations

A single pre-industrial Holocene (PI) vegetation simulation was obtained by driving BIOME4 with contemporary climate but with CO_2 concentration set at the pre-industrial value of 280 ppm. Palaeo-simulations with BIOME4 were obtained after adding anomalies (differences between simulated palaeo- and control model runs) of monthly climate variables to the contemporary climate baseline. We generated climate-model anomaly fields for each monthly mean climate variable (12 variables for temperature, 12 for precipitation and 12 for fractional sunshine hours) and interpolated these to the BIOME4 grid. Absolute minimum temperature values, required by BIOME4 to locate the boundary between tropical and non-tropical woody biomes, were adjusted from modern values by finding the coldest month separately for each grid cell in the climate dataset and applying the anomaly of the monthly minimum temperature values for that month to the modern absolute minimum temperature. The entire procedure was carried out separately using the output of each climate model.

A CO_2 concentration of 280 ppm was prescribed for all the MH runs of BIOME4 and also for LGM climate-only runs, to demonstrate the effect of changing to a glacial climate without lowering CO_2. For the full LGM runs, a CO_2 concentration of 189 ppm was precribed. The value of 189 ppm was chosen because it represents the average of ice-core measurements of the CO_2 concentration in MIS 2 (Petit et al., 1999).

2.3 Modelling stable carbon isotope composition

BIOME4 simulates average ^{13}C discrimination by vegetation (Kaplan et al., 2002). The ^{13}C computation is summarized in Appendix A. It accounts both for changes in the balance of C_3 and C_4 plants, which can be influenced by CO_2 concentration, temperature and moisture availability, and changes in stomatal conductance related to moisture availability in C_3 plants. Observed large-scale spatial variations in tissue δ^{13}C at the leaf level, respired CO_2 at the ecosystem level, and latitudinal variations in the δ^{13}C values of biospheric CO_2 sources and sinks contributing to measured seasonal cycles of $\delta^{13}CO_2$ in the atmosphere, can all be well simulated using this scheme (Kaplan et al., 2002).

2.4 Estimating and applying source areas

The prevailing winds today track consistently from east to west across subequatorial Africa. PMIP simulations for subequatorial Africa show only slight changes in wind strength and direction across Africa from LGM to MH and recent times, except in the southernmost part of the continent (Braconnot et al., 2007). We therefore used modern wind trajectory data to approximate the past and present continental source areas of each marine core. Each marine core location was subjected to a back-trajectory wind analysis using the HYSPLIT tool, available at the National Oceanic and Atmospheric Administration's Real-time Environmental Applications and Display sYstem (READY) website, http://www.arl.noaa.gov/ready/hysplit4.html. Altogether 216 trajectories (6 yr × 12 months × 3 heights) were obtained for each core location tracking back for 5 days (see Supplement Fig. S1). Probabilities for each 0.5° grid cell in the region considered were obtained as frequencies for each trajectory to pass over the grid cell based on the method of Lunt et al. (2001), then weighted by leaf area index for the cell to account for spatial variations in the amount of leaf material available for deflation.

As a simple alternative and robustness test, we considered latitude bands, 5° wide, extending from the west coast to 30° E, centred on the latitude of each core, with weighting again by leaf area index but with all grid cells in the band considered to have an equal probability of being a source. The results (not shown) were nearly identical.

Isotopic values for each core location, simulated as described above, were converted to represent *n*−alkane values by applying the average offset values from Collister et al. (1994), linearly interpolated between the end-member values for C_3 and C_4 plants according to the relative amounts of modelled C_3 and C_4 vegetation in the grid cells. Background (air) δ^{13}C values were taken to be −6.52 ‰ in the PI and MH and −6.66 ‰ at the LGM (Indermühle et al., 1998; Smith et al., 1999), a difference with only a very minor impact.

2.5 Modelling biomes and comparison with pollen data

To supplement the analysis based on stable isotopes, we considered changes in biome distributions as modelled by BIOME4 and represented in pollen records. These are however sparse for Africa, especially in the tropics. Elenga et al. (2000) presented the most recent synthesis of LGM and MH pollen data for Africa. We simplified the biome classifications at the pollen sites as given by Elenga et al. (2000) by aggregating to broad classes using the scheme of Prentice et al. (2011a). Additional BIOME4 simulations based on the average climate anomalies simulated by the LGM and MH models were carried out in order to construct palaeo-biome maps for comparison, using the output classification of Prentice et al. (2011a) to allow direct comparability between the modelled and reconstructed biome classifications.

3 Results

The PI simulation shows a north-south profile close to the Holocene observations of *n*-alkane δ^{13}C, with values in the range of −24 to −28 ‰ in the southern part of the transect is shown in Fig. 2a. North of 20° S both the observed and modelled values become progressively more negative with decreasing latitude, reaching −32 to −35 ‰

at 5° S. The MH simulation is close to the PI simulation, indicating that the simulated Holocene vegetation changes in this region were minor, compared to those between LGM and Holocene. As the δ^{13}C measurements represent composite sediment samples from a broad time period within MIS 1, they include material representing MH as well as more recent times. The simulated MH δ^{13}C values for 5 to 7° S (−32 to −33 ‰) are closer to the observed values than the simulated PI values. The differences are small in any case.

The LGM data occupy a similar range of δ^{13}C values to the Holocene values in the southern part of the transect. North of 20° S they diverge, becoming more negative but less steeply than in the Holocene, reaching only to −30 ‰ by 5° S is shown in Fig. 2a. In contrast, the simulated LGM values based on climate change alone remain close to the observed Holocene – not LGM – values. This finding shows that climate change alone (including the effects of changes in moisture availability on ^{13}C discrimination by C_3 plants, which is explicitly modelled) cannot explain the observed change in ^{13}C discrimination between the LGM and Holocene.

Only when realistic LGM CO_2 concentration is applied in the biome simulation do the simulated tropical values show the observed LGM pattern, reaching a value identical to the observed LGM δ^{13}C value at 5° S. The disparity is seen most clearly in Fig. 2b, which shows the (LGM minus Holocene) differences in the observed δ^{13}C values, and the corresponding differences (LGM minus PI) in the simulated δ^{13}C values. North of 20° S, the differences based on the full LGM simulation (with climate change and realistic CO_2 concentration) remain close to the differences seen in the data. Observed and simulated differences are in the range 3.5 ± 1.5 ‰. The differences based on the "climate only" LGM simulation are in the range of 0 ± 1 ‰ only, and do not overlap at all with the observed range of differences.

A similar contrast can be seen in the simulated biome distributions in Fig. 3a. The LGM climate-only simulation shows a slight expansion of tropical forests whereas the full LGM simulation with realistic CO_2 concentration shows a substantial contraction of forests, with grasslands and dry shrublands expanding to largely replace both savanna and forests north of 20° S. The limited available pollen data for comparison (Jolly et al., 1998; Elenga et al., 2000) are summarized in Fig. 3b. The data are too sparse to allow the simulations to be evaluated unequivocally, but they are consistent with the model results. The pollen data show a reduction in the incidence of tropical forests at LGM in the region of the East African Rift Great Lakes, which is modelled by the full LGM simulation with realistic CO_2 concentration but not by the climate-only LGM simulation. The pollen data also support the model predictions of little change between MH and today, and no major biome shifts south of 20° S between the LGM and MH.

4 Discussion

These results show that the glacial-interglacial climate change, as simulated by the range of PMIP models, cannot account for observed stable carbon isotope and vegetation changes in tropical southern Africa. The models show reduced precipitation at the LGM, which is consistent with previous analyses. But the effects of reduced precipitation are not large enough to explain the δ^{13}C measurements or the pollen records. This lack of a strong effect of reduced precipitation can be explained as a consequence of countervailing effects of lower temperatures in reducing evapotranspiration (conserving soil moisture) and photorespiration (allowing greater C_3 plant productivity than would otherwise be possible at low CO_2 concentration) (Cowling and Shin, 2006). On the other hand, the effects of CO_2 concentration as modelled by BIOME4, in combination with the climate change effects, are consistent with the δ^{13}C data. The modelled effect of CO_2 concentration is a consequence of the strong dependence of C_3 photosynthesis on CO_2 concentration in the subambient range (Polley et al., 1993; Cowling and Sage, 1998; Harrison and Bartlein, 2011) contrasting with the relatively weak effect of CO_2 concentration on plants with C_4 photosynthesis. This finding points to a key role of atmospheric CO_2 concentration in determining glacial-interglacial biome distribution changes in the tropics.

There are important implications for the interpretation of palaeo-δ^{13}C measurements. *n*-alkane δ^{13}C data from another African margin transect that crosses the equator, extending between 20° N and 20° S, have been interpreted in terms of climate change only (Colins et al., 2011). The similarity of observed LGM-to-Holocene δ^{13}C shifts in the northern and southern hemispheres was interpreted as evidence for symmetrical changes in the distribution of rainfall around the equator (Colins et al., 2011). But the long-standing empirical evidence for CO_2 concentration effects on the balance of C_3 trees and C_4 grasses (Bond and Midgley, 2000) contradicts the explicit assumption in Collins et al. (2011) that this balance is controlled by hydrology alone. In contrast, Sinninghe Damsté et al. (2011) presented *n*-alkane δ^{13}C values from an East African lake core, with much higher temporal resolution than can normally be achieved with marine sediments, and concluded that “rainfall variation by itself is not the single most important driver of long-term vegetation change in this region of tropical Africa... the relatively invariant C_3 / C_4 ratio during the glacial and Holocene periods resembles the main long-term trend in atmospheric pCO_2, suggesting substantial control” (Sinninghe Damsté et al., 2011). With knowledge of CO_2 effects, apparently symmetrical “expansion of the African rainbelt” from glacial to Holocene periods (Collins et al., 2011) can be re-interpreted as a direct consequence of forcing by changes in atmospheric CO_2 concentration, which is bound to be symmetrical because the effects are global, evoking similar responses in the northern and southern hemispheres. Unlike the interpretation of Collins et al. (2011), this re-interpretation of the data does not contradict previous interpretations (and model simulations) that indicate a northward shift of the African rainbelt from the LGM to Holocene.

Finally, these results have implications for the interpretation of the worldwide trend towards increased tree density in savannas, known as “woody thickening”. The effect of CO_2 concentration on photosynthesis in C_3 plants, including trees, is steeper in the lower range than in the present range, but it is still substantial (Cowling and Sage, 1998). By a conservative calculation, assuming a ratio of internal leaf to ambient CO_2 concentration of 0.7, and co-limitation of C_3 photosynthesis by Rubisco and electron transport, an increase of CO_2 concentration from 280 ppm to 380 ppm should have increased the potential growth rates of C_3 plants during the industrial era by ∼15 to 20 %. A continued increase from 380 ppm to 550 ppm should cause a further increase of similar magnitude in the potential growth rates of C_3 plants. Given the weak response of C_4 photosynthesis (as used by tropical grasses) to CO_2 concentration, this increase in C_3 photosynthesis would be expected to increase the competitive ability of C_3 plants and thereby influence the balance of C_3 and C_4 plant dominance. The effect should be noticeable even if the CO_2 effect is partially counteracted by other constraints, such as nitrogen limitation and the associated diversion of primary production to root growth (Palmroth et al., 2006; Finzi et al., 2007). In dry environments the effect of rising CO_2 concentration is likely to be even greater than this simple calculation suggests, because stomata are more closed (conserving water) in dry environments and so a change in CO_2 has a proportionally larger effect.

Our findings do not rule out a contribution to contemporary woody thickening from other factors including land-use change (Archer et al., 1995) but they indicate that continued rise in CO_2 concentration is nonetheless likely to further increase woody plant cover today, just as it did during the worldwide reforestation after the LGM. And whereas the transition from LGM to Holocene has to be understood through reconstruction and modelling, the specific effects of changes from present CO_2 levels are amenable to experiments – not only FACE experiments, which are expensive, but also experiments that could be conducted on a more modest scale to analyse the responses of ecosystems in controlled environments.

Appendix A

Isotopic discrimination in the BIOME4 model

BIOME4 (Kaplan, 2001; Kaplan et al., 2003) is an equilibrium model for large-scale biome distribution based on the comparison of potential net primary production (NPP) for plant functional types (PFTs) that differ in stature, phenology, physiology and bioclimatic requirements. NPP is modelled as a balance of photosynthesis and respiration, allowing the computation of ancillary properties such as the leaf-internal CO_2 concentration (c_i), needed to quantify the discrimination against ^{13}C during photosynthesis (Kaplan et al., 2002). The set of 12 PFTs considered includes various types of (C_3) trees, and both C_4 and C_3 herbaceous plants. Bioclimatic limits provide a coarse environmental filter so that, for example, tropical trees are confined to frost-free climates. Among PFTs allowed by the filter, by default the dominant PFT is chosen to be the tree type with the highest NPP. However under dry conditions (below an empirically determined threshold value of soil moisture content) herbaceous PFTs are allowed to "compete" with trees; the dominant PFT is then simply the one with the highest NPP. The δ^{13}C value output by the model applies to the dominant PFT in forests, but is a flux-weighted average of values for the woody and herbaceous PFTs present in mixtures.

Among C_3 plants, each PFT is assigned a maximum value of the ratio $c_\mathrm{i}/c_\mathrm{a}$ where c_a is ambient CO_2 concentration. These maximum values were determined by a literature review. The rate of transpiration (E) is the lesser of an evaporative demand term (D) and a supply term (S). The maximum $c_\mathrm{i}/c_\mathrm{a}$ ratios apply so long as $E = D$:

$$D = \alpha_m E_\mathrm{q}[1 - exp(g_\mathrm{p}/g_\mathrm{o})] \tag{A1}$$

where $\alpha_m = 1.4$, E_q is the equilibrium rate of evapotranspiration (a function of net radiation and temperature only), g_p is "potential stomatal" conductance (i.e. the value that yields the maximum $c_\mathrm{i}/c_\mathrm{a}$ ratio) and g_o is a scaling parameter. $c_\mathrm{i}/c_\mathrm{a}$ ratios are reduced when $E = S$:

$$S = w \cdot E_\mathrm{m} \tag{A2}$$

where w ($0 \le w \le 1$) is relative volumetric soil moisture (a weighted average of the two soil layers, with weighting determined by the specified vertical root profile for the PFT) and E_m is a PFT-specific maximum transpiration rate. Under these conditions, stomatal conductance g_s is determined by the general case of Eq. (1):

$$E = \alpha_m E_q[1 - exp(g_s/g_o)] \tag{A3}$$

where E is now determined from Eq. (2), yielding

$$g_s = g_o / n[1/(1-\alpha^*)] \tag{A4}$$

where

$$\alpha^* = E/\alpha_m E_q \tag{A5}$$

c_i is then calculated by simultaneous solution of the biochemical and diffusion equations for photosynthesis. Discrimination against ^{13}C is calculated from c_i/c_a following Lloyd and Farquhar (1994):

$$\Delta = 1.9 - 8\Gamma^*/c_a + 23.1 c_i/c_a \tag{A6}$$

with $\Gamma^* = 1.54T$, where T is an estimate of daytime leaf temperature in °C.

Ecosystem Δ values are averages over PFTs, weighted by the gross primary production of each PFT. Discrimination by C_4 photosynthesis is always less than discrimination by C_3 photosynthesis, and is only weakly sensitive to environment. Kaplan et al. (2002) showed that this scheme gives good respresentations of the large-scale patterns of observed $\delta^{13}C$ values at the level of individual leaf samples, at the ecosystem level based on measurements of respired CO_2, and at the regional level based on "Keeling plots" of $\delta^{13}CO_2$ versus $1/[CO_2]$.

Supplementary material related to this article is available online at: http://www.biogeosciences-discuss.net/9/15699/2012/ bgd-9-15699-2012-supplement.pdf.

Acknowledgements. We acknowledge the international modelling groups for providing their data for analysis and the Laboratoire des Sciences du Climat et de l'Environnement (LSCE) for collecting and archiving the model data. The PMIP2/MOTIF Data Archive has been supported by CEA, CNRS, the EU project MOTIF (EVK2-CT-2002-00153) and the Programme National d'Etude de la Dynamique du Climat (PNEDC). More information about the PMIP archive is available at: http://pmip2.lsce.ipsl.fr/.

References

Ainsworth, E. A. and Piao, S. L.: What have we learned from 15 years of free-air CO_2 enrichment (FACE)? A meta-analytic review of the responses of photosynthesis, canopy properties and plant production to rising CO_2, New Phytol., 165, 351–372, 2005.

Archer, S., Boutton, T. W., and Hibbard, K. A.: Trees in grasslands: biogeochemical consequences of woody plant expansion, in: Global Biogeochemical Cycles in the Climate System, edited by: Schulze, E.-D., Heimann, M., Harrison, S., Holland, E., Lloyd, J., Prentice, I. C., and Schimel, D., Academic Press, San Diego, 115, 2001.

Archer, S., Schimel, D. S., and Holland, E. A.: Mechanisms of shrubland expansion: land use, climate or CO_2? Climatic Change, 29, 91–99, 1995.

Bond, W. J.: What limits trees in C_4 grasslands and savannas? Annu. Rev. Ecol. Evol. Syst., 39, 641–659, 2008.

Bond, W. J. and Midgley, G. F.: A proposed CO_2-controlled mechanism of woody plant invasion in grasslands and savannas, Glob. Change Biol., 6, 865–869, 2000.

Bond, W. J., Midgley, G. F., and Woodward, F. I.: The importance of low atmospheric CO_2 and fire in promoting the spread of grasslands and savannas, Glob. Change Biol., 9, 973–982, 2003.

Braconnot, P., Otto-Bliesner, B., Harrison, S., Joussaume, S., Peterchmitt, J.-Y., Abe-Ouchi, A., Crucifix, M., Driesschaert, E., Fichefet, Th., Hewitt, C. D., Kageyama, M., Kitoh, A., Laîné, A., Loutre, M.-F., Marti, O., Merkel, U., Ramstein, G., Valdes, P., Weber, S. L., Yu, Y., and Zhao, Y.: Results of PMIP2 coupled simulations of the Mid-Holocene and Last Glacial Maximum – Part 1: experiments and large-scale features, Clim. Past, 3, 261–277, doi:10.5194/cp-3-261-2007, 2007.

Collins, J. A., Schefuß, E., Heslop, D., Mulitza, S., Prange, M., Zabel, M., Tjallingii, R., Dokken, T. M., Huang, E., Mackensen, A., Schulz, M., Tian, J., Zarriess, M., and Wefer, G.: Interhemispheric symmetry of the tropical African rainbelt over the past 23,000 years, Nat. Geosci., 4, 42–45, 2011.

Collister, J. W., Rieley, G., Stern, B., Eglinton, G., and Fry, B.: Compound-specific δ^{13}C analyses of leaf lipids from plants with differing carbon dioxide metabolisms, Org. Geochem. 21, 619–627, 1994.

Cowling, S. A.: Simulated effects of low atmospheric CO_2 on structure and composition of North American vegetation at the Last Glacial Maximum, Global Ecol. Biogeogr., 8, 81–93, 1999.

Cowling, S. A. and Sage, R. F.: Interactive effects of low atmospheric CO_2 and elevated temperature on growth, photosynthesis and respiration in Phaseolus vulgaris, Plant Cell Env., 21, 427–435, 1998.

Cowling, S. A. and Shin, Y.: Simulated ecosystem threshold responses to co-varying temperature, precipitation and atmospheric CO_2 within a region of Amazonia, Global Ecol. Biogeogr., 15, 553–566, 2006.

Cowling, S. A. and Sykes, M. T.: Physiological significance of low atmospheric CO_2 for plant-climate interactions, Quat. Res., 52, 237–242, 1999.

Diefendorf, A. F., Mueller, K. E., Wing, S. L., Koch, P. L., and Freeman, K. H.: Global patterns in leaf ^{13}C discrimination and implications for studies of past and future climate, P. Natl. Acad. Sci. USA., 107, 5738–5743, 2010.

Eglinton, T. I. and Eglinton, G.: Molecular proxies for paleoclimatology. Earth Planet. Sci. Lett., 275, 1–16, 2008.

Ehleringer, J. R., Cerling, T. E., and Helliker, B. R.: C_4 photosynthesis, atmospheric $CO_2$and climate, Oecologia, 112, 285–299, 1997.

Elenga, H., Peyron, O., Bonnefille, R., Jolly, D., Cheddadi, R., Guiot, J., Andrieu, V., Bottema, S., Buchet, G., de Beaulieu, J.-L., Hamilton, A. C., Maley, J., Marchant, R., Perez-Obiol, R., Reille, M., Riollet, G., Scott, L., Straka, H., Taylor, D., Van Campo, E., Vincens, A., Laarif, F., and Jonson, H.: Pollen-based biome reconstruction for southern Europe and Africa 18,000 yr BP, J. Biogeogr., 27, 621–634, 2000.

Farquhar, G. D.: On the nature of carbon isotope discrimination in C_4 species, Aust. J. Plant Physiol., 10, 205–226, 1983.

Farquhar, G. D., O'Leary, M. H., and Berry, J. A.: On the relationship between carbon isotope discrimination and the intercellular carbon dioxide concentration in leaves, Aust. J. Plant Physiol., 9, 121–137, 1982.

Finzi, A. C., Norby, R. J., Calfapietra, C., Gallet-Budynek, A., Gielen, B., Holmes, W. E., Hoosbeek, M. R., Iversen, C. M., Jackson, R. B., Kubiske, M. E., Ledford, J., Liberloo, M., Oren, R., Polle, A., Pritchard, S., Zak, D. R., Schlesinger, W. H., and Ceulemans, R.: Increases in nitrogen uptake rather than nitrogen-use efficiency support higher rates of temperate forest productivity under elevated CO_2, P. Natl. Acad. Sci. USA, 104, 14014–14019, 2007.

Friedlingstein, P., Cox, P., Betts, R., Bopp, L., von Bloh, W., Brovkin, V., Cadule, P., Doney, S., Eby, M., Fung, I., Bala, G., John, J., Jones, C., Joos, F., Kato, T., Kawamiya, M., Knorr, W., Lindsay, K., Mattews, H. D., Raddatz, T., Rayner, P., Reick, C., Roeckner, E., Schnitzler, K.-G., Schnur, R., Strassmann, K., Weaver, A. J., Yoshikawa, C., and Zeng, N.: Climate-carbon cycle feedback analysis: Results from the C^4MIP model intercomparison, J. Climate, 19, 3337–3353, 2006.

Harrison, S. P. and Bartlein, P. J.: Records from the past, lessons for the future: what the palaeorecord implies about mechanisms of global change, in: The Future of the World's Climate, edited by: Henderson-Sellers, A. and McGuffie, K., Elsevier, 1103, 2011.

Harrison, S. P. and Prentice, I. C.: Climate and CO_2 controls on global vegetation distribution at the last glacial maximum: analysis based on palaeovegetation data, biome modelling and palaeoclimate simulations, Glob. Change Biol., 9, 983–1004, 2003.

Indermühle, A., Stocker, T. F., Joos, F., Fischer, H., Smith, H. J., Wahlen, M., Deck, B., Mastroianni, D., Tschumi, J., Blunier, T., Meyer, R., and Stauffer, B.: Holocene carbon-cycle dynamics based on CO_2 trapped in ice at Taylor Dome, Antarctica, Nature, 398, 121–126, 1998.

Jolly, D. and Haxeltine, A.: Effect of low glacial atmospheric CO_2 on tropical African montane vegetation, Science, 276, 786–788, 1997.

Jolly, D., Prentice, I. C., Bonnefille, R., Ballouche, A., Bengo, M., Brenac, P., Buchet, G., Burney, D., Cazet, J.-P., Cheddadi, R., Edorh, T., Elenga, H., Elmoutaki, S., Guiot, J., Laarif, F., Lamb, H., Lezine, A.-M., Maley, J., Mbenza, M., Peyron, O., Reille, M., Reynaud-Farrera, I., Riollet, G., Ritchie, J. C., Roche, E., Scott, L., Ssemmanda, I., Straka, H., Umer, M., Van Campo, E., Vilimumbalo, S., Vincens, A., and Waller, M.: Biome reconstruction from pollen and plant macrofossil data for Africa and the Arabian peninsula at 0 and 6000 years, J. Biogeogr., 25, 1007–1027, 1998.

Kaplan, J. O.: Geophysical applications of vegetation modeling, Ph.D. thesis, Lund University, 2001.

Kaplan, J. O., Prentice, I. C., and Buchmann, N.: The stable carbon isotope composition of the terrestrial biosphere: modelling at scales from the leaf to the globe, Global Biogeochem. Cy., 16, GB1060, doi:10.1029/2001GB001403, 2002.

Kaplan, J. O., Bigelow, N. H., Prentice, I. C., Harrison, S. P., Bartlein, P. J., Christensen, T. R., Cramer, W., Matveyeva, N. V., McGuire, A. D., Murray, D. F., Razzhivin, V. Y., Smith, B., Walker, D. A., Anderson, P. M., Andreev, A. A., Brubaker, L. B., Edwards, M. E., and Lozhkin, A. V.: Climate change and Arctic ecosystems II: Modeling, paleodata-model comparisons and future projections, J. Geophys. Res., 108, 8171, doi:10.1029/2002JD002559, 2003.

Kgope, B. S., Bond, W. J., and Midgley, G. F.: Growth responses of African savanna trees implicate atmospheric $[CO_2]$ as a driver of past and current changes in savanna tree cover, Austral Ecol., 35, 451–463, 2010.

Lloyd, J. J. and Farquhar, G. D.: ^{13}C discrimination during CO_2 assimilation by the terrestrial biosphere, Oecologia, 99, 201–215, 1994.

Lunt, D. J. and Valdes, P. J.: Dust transport to Dome C, Antarctica, at the Last Glacial Maximum and present day, Geophys. Res. Lett., 28, 295–298, doi:10.1029/2000GL012170, 2001.

Macinnis-Ng, C., Zeppel, M., Williams, M., and Eamus, D.: Applying a SPA model to examine the impact of climate change on GPP of open woodlands and the potential for woody thickening, Ecohydrology, 4, 379–393, 2011.

Norby, R. J., DeLucia, E. H., Gielen, B., Calfapietra, C., Giardina, C. P., King, J. S., Ledford, J., McCarthy, H. R., Moore, D. J. P., Ceulemans, R., De Angelis, P., Finzi, A. C., Karnosky, D. F., Kubiske, M. E., Lukac, M., Pregitzer, K. S., Scarascia-Mugnozza, G. E., Schlesinger, W. H., and Oren, R.: Forest response to elevated CO_2 is conserved across a broad range of productivity, P. Natl. Acad. Sci. USA, 102, 18052–18056, 2005.

Palmroth, S., Oren, R., McCarthy, H. R., Johnsen, K. H., Finzi, A. C., Butnor, J. R., Ryan, M. G., and Schlesinger, W. H.: Aboveground sink strength in forests controls the allocation of carbon below ground and its $[CO_2]$-induced enhancement, P. Natl. Acad. Sci. USA, 103, 19362–19367, 2006.

Pearson, A. and Eglinton, T. I.: The origin of n-alkanes in Santa Monica Basin surface sediment: a model based on compound-specific Δ^{14}C and δ^{13}C data, Org. Geochem., 31, 1103–1116, 2000.

Title Page
Abstract Introduction
Conclusions References
Tables Figures
◀| |▶
◀ ▶
Back Close
Full Screen / Esc
Printer-friendly Version
Interactive Discussion

Peltier, W. R.: Global glacial isostasy and the surface of the ice-age Earth: the ICE-5G (VM2) model and GRACE, Annu. Rev. Earth Planet. Sc., 32, 111–149, 2004.

Petit, J. R., Jouzel, J., Raynaud, D., Barkov, N. I., Barnola, J.-M., Basile, I., Bender, M., Chappellaz, J., Davis, M., Delaygue, G., Delmotte, M., Kotlyakov, V. M., Legrand, M., Lipenkov, V. Y., Lorius, C., Pépin, L., Ritz, C., Saltzman, E., and Stievenard, M.: Climate and atmospheric history of the past 420,000 years from the Vostok ice core, Antarctica, Nature, 399, 429–436, 1999.

Polley, H. W., Johnson, H. B., Marino, B. D., and Mayeux, H. S.: Increases in C_3 plant water-use efficiency and biomass over Glacial to present CO_2 concentrations, Nature, 361, 61–64, 1993.

Prentice, I. C. and Harrison, S. P.: Ecosystem effects of CO_2 concentration: evidence from past climates, Clim. Past, 5, 297–307, doi:10.5194/cp-5-297-2009, 2009.

Prentice, I. C., Farquhar, G. D., Fasham, M. J. R., Goulden, M. L., Heimann, M., Jaramillo, V. J., Kheshgi, H. S., Le Quéré, C., Scholes, R. J., Wallace, D. W. R., Archer, D., Ashmore, M. R., Aumont, O., Baker, D., Battle, M., Bender, M., Bopp, L. P., Bousquet, P., Caldeira, K., Ciais, P., Cox, P. M., Cramer, W., Dentener, F., Enting, I. G., Field, C. B., Friedlingstein, P., Holland, E. A., Houghton, R. A., House, J. I., Ishida, A., Jain, A. K., Janssens, I. A., Joos, F., Kaminski, T., Keeling, C. D., Keeling, R. F., Kicklighter, D. W., Kohfeld, K. E., Knorr, W., Law, R., Lenton, T., Lindsay, K., Maier-Reimer, E., Manning, A. C., Matear, R. J., McGuire, A. D., Melillo, J. M., Meyer, R., Mund, M., Orr, J. C., Piper, S., Plattner, K., Rayner, P. J., Sitch, S., Slater, R., Taguchi, S., Tans, P. P., Tian, H. Q., Weirig, M. F., Whorf, T., and Yool, A.: The carbon cycle and atmospheric carbon dioxide, in: Climate Change 2001: The Scientific Basis, edited by: Houghton, J. T., Ding, Y., Griggs, D. J., Noquer, M., van der Linden, P. J., Dai, X., Maskell, K., and Johnson, C. A., Cambridge University Press, Cambridge, UK, 183–224, 2001.

Prentice, I. C., Harrison, S. P., and Bartlein, P. J.: Global vegetation and terrestrial carbon cycle changes after the last ice age, New Phytol., 189, 988–998, 2011a.

Prentice, I. C., Meng, T., Wang, H., Harrison, S. P., Ni, J., and Wang, G.: Evidence of a universal scaling relationship for leaf CO_2 drawdown along an aridity gradient, New Phytol., 190, 169–180, 2011.

Rommerskirchen, F., Eglinton, G., Dupont, L., and Rullkötter, J.: Glacial/interglacial changes in southern Africa: Compound-specific $\delta^{13}C$ land plant biomarker and pollen records from southeast Atlantic continental margin sediments, Geochem. Geophys. Geosyst., 7, Q08010, doi:10.1029/2005GC001223, 2006.

Sinninghe Damsté, J. S., Verschuren, D., Ossebaar, J., Blokker, J., van Houten, R., Plessen, B., and Schouten, S.: A 25,000-year record of climate-induced changes in lowland vegetation of eastern equatorial Africa revealed by the stable carbon-isotopic composition of fossil plant leaf waxes, Earth Planet. Sci. Lett., 302, 236–246, 2011.

Smith, H. J., Fischer, H., Wahlen, M., Mastroianni, D., and Deck, B.: Dual modes of the carbon cycle since the Last Glacial Maximum, Nature, 400, 248–250, 1999.

Street-Perrott, F. A., Huang, Y., Perrott, R. A., Eglinton, G., Barker, P., Khelifa, L. B., Harkness, D. D., and Olago, D. O.: Impact of lower atmospheric carbon dioxide on tropical mountain ecosystems, Science, 278, 1422–1426, 1997.

Vogts, A.: Plant wax alkanes and alkan-1-ols in ocean sediments as indicators of continental climate change – validation of a molecular proxy, Ph.D. thesis, University of Oldenburg, Germany, available at: http://oops.uni-oldenburg.de/volltexte/2011/1192, 2011.

Vogts, A., Schefuß, E., Badewien, T., and Rullkötter, J.: *n*-Alkane parameters derived from a deep-sea sediment transect off southwest Africa reflect continental vegetation and climate conditions, Org. Geochem., 47, 109–119, 2012.

Zhao, M., Dupont, L., Eglinton, G., and Teece, M.: *n*-Alkane and pollen reconstruction of terrestrial climate and vegetation for N.W. Africa over the last 160 kyr, Org. Geochem., 34, 131–143, 2003.

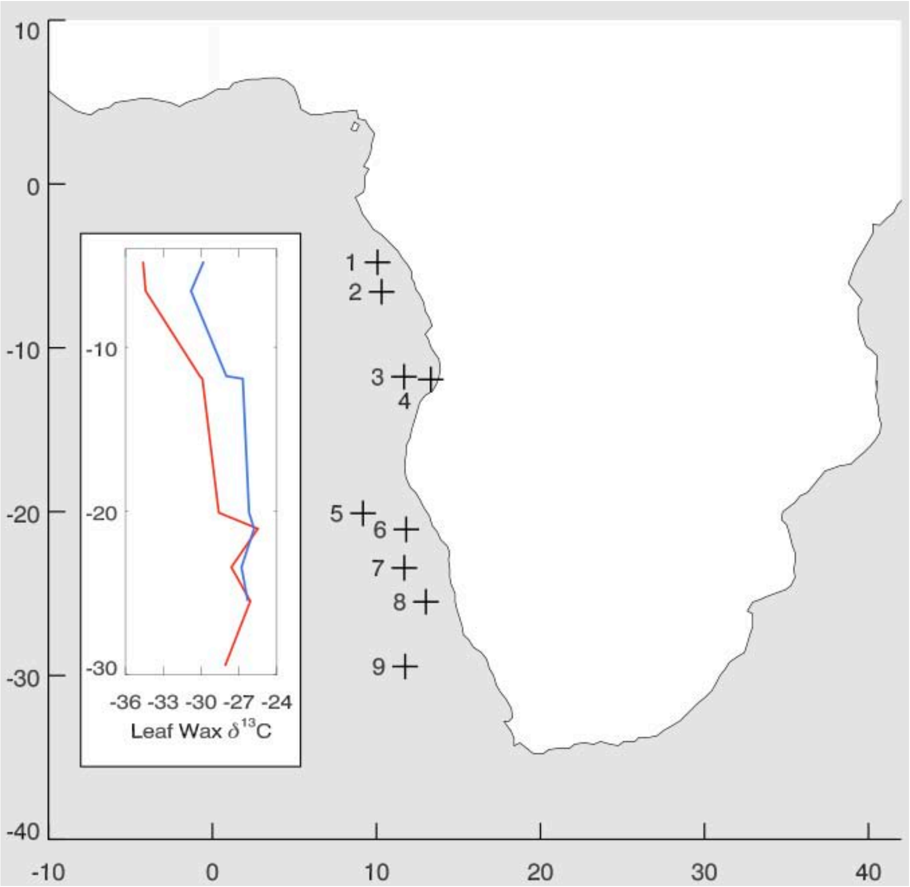

Fig. 1. Locations of the marine core sites, and the δ^{13}C data of leaf-wax *n*-alkanes extracted from Holocene (red) and LGM (blue) sediments as a function of latitude. Data from Rommerskirchen et al. (2006).

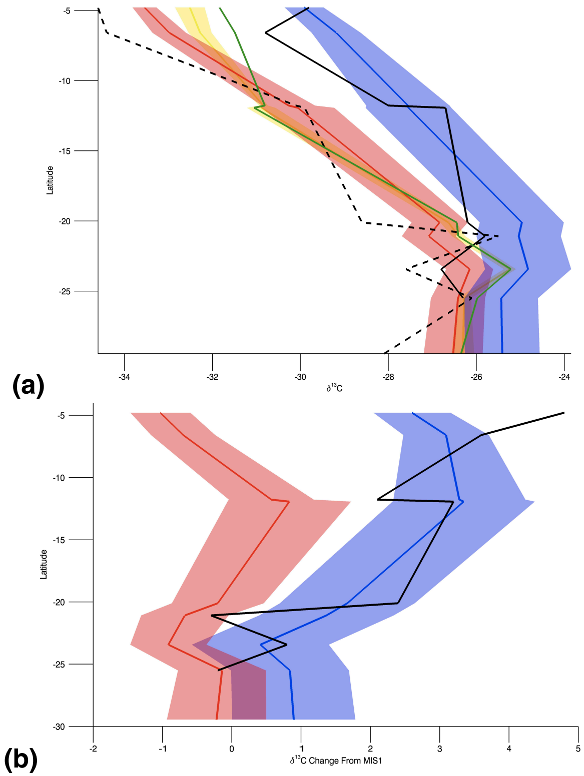

Fig. 2. (a) Observed and simulated δ^{13}C values of leaf wax *n*-alkanes at the core sites as a function of latitude. Dashed black line: Holocene data, solid black line: LGM data. Simulations: PI (green), MH (yellow), LGM with pre-industrial CO_2 (280 ppm, red), and LGM with realistic CO_2 (189 ppm, blue). **(b)** Observed and simulated differences in δ^{13}C values of leaf wax *n*-alkanes. Black line: data, LGM minus Holocene. Simulations: LGM with pre-industrial CO_2 minus PI (red); LGM with realistic CO_2 minus PI (blue). In both panels, simulated values are shown as means (coloured lines) and ranges (shading) across climate models.

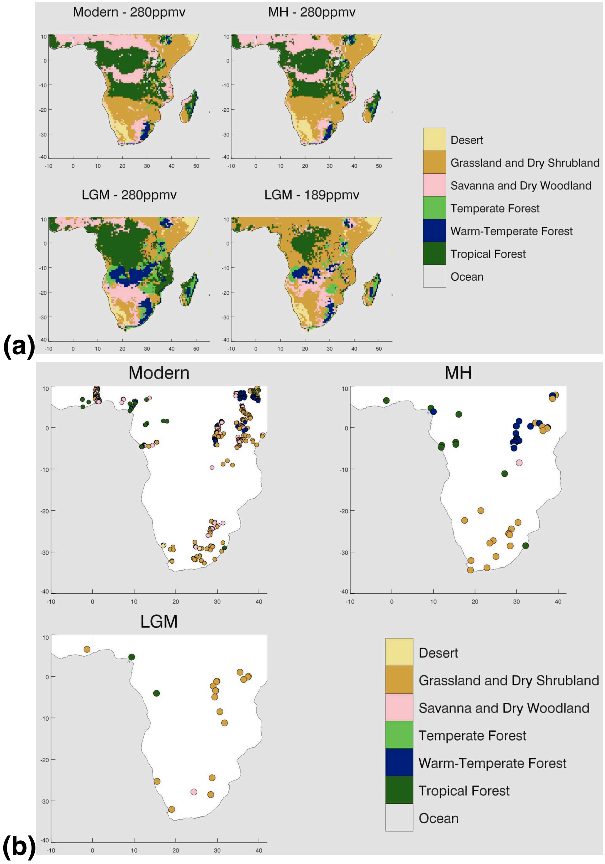

Fig. 3. (a) Simulated biome distributions for PI, MH (model-average climate), LGM (model-average climate and pre-industrial CO_2, 280 ppm) and LGM (model-average climate and realistic CO_2, 189 ppm). **(b)** Biomes assigned to pollen data for PI (surface samples), MH and LGM.